VAMP2 (Fig. 2C). To further characterize the distribution of DJ-1 within synaptosomes, we investigated members of the family of monomeric GTPases called Rab proteins, such as Rab3A (exocytosis marker), Rab4A (recycling marker), Rab5B (endosome marker), and Rab7B (late endosome marker). As shown in Fig. 2B, these Rab proteins co-fractionated with DJ-1. However, mitochondrial respiratory complex proteins (Complex I subunit NDUFB8, Complex II subunit 30 kDa, Complex III subunit Core 2, and ATP synthase (Complex V) subunit α), which are mitochondrial markers, and the Golgi apparatus protein GM130, were not concentrated in the synaptic vesicle fraction (LP2) (Fig. 2D). The amount of each fraction was quantified and expressed as a percentage for the estimated amount of whole brain protein. The percentage of the P1 fraction was $2.69 \pm 0.20\%$, and DJ-1 was present in the nucleus, even though it was small. The percentages of P2′, LS1, LP1, LS2, and LP2, were $19.07 \pm 0.80\%$, $3.71 \pm 0.08\%$, $17.58 \pm 2.36\%$, $2.46 \pm 0.11\%$, and $0.75 \pm 0.19\%$, respectively (Fig. 2E). The amount of protein in the LP2 fraction was much less than that of the whole brain. DJ-1 IR of each fraction was quantified and shown as a percentage of each IR to total immunoreactivities. The percentage of DJ-1 IR of each fraction was $9.82 \pm 0.22\%$ (P2′), $13.19 \pm 0.07\%$ (LS1), $6.18 \pm 0.20\%$ (LP1), $12.54 \pm 0.50\%$ (LS2), and $5.43 \pm 1.08\%$ (LP2) (Fig. 2F).

DJ-1 localized on synaptic vesicles associated with synaptophysin and Rab3A

DJ-1 distributed with synaptic vesicles in the mouse brain (Fig. 2C). To elucidate the vesicle localization of DJ-1, the LS1 fraction containing synaptic vesicles and cytosol from mouse brain was further fractionated by sucrose density gradients centrifugation. Synaptophysin, VAMP2, synaptotagmin, and several Rab proteins were seen in fractions 9–18, and therefore, synaptic vesicles were collected in these fractions (Fig. 3A, B). Otherwise, the immunoreactivities of the synaptic vesicle markers were absent in fractions 1–8, suggesting that they were cytosolic fractions. The distribution of DJ-1 displayed biphasic peaks of both cytosolic fractions (fractions 1–8) and vesicle fractions (fractions 12–14). Coincidentally, the peak of DJ-1 IR agreed with the latter peak of synaptophysin and Rab3A (Fig. 3A, B). To further investigate the colocalization between DJ-1 and synaptic vesicles in neurons, primary cortical neuronal cells obtained from mouse brain were double-stained for DJ-1, and for synaptophysin or Rab3A. DJ-1 immunostaining appeared as punctate structures in the cytosol, axon, and synaptic terminals. DJ-1 was found to partly colocalize with synaptophysin and Rab3A, which play important roles in exocytosis (Edelmann et al., 1995; Handley et al., 2007) (Fig. 3C).

To gain further insight into the vesicle localization of DJ-1, immunoisolation was performed, as previously described (Burre et al., 2007; Morciano et al., 2005), with the LS1 fraction containing synaptic cytosol and vesicles from the mouse brain (Fig. 4A). To remove the nonspecifically interacting material, the LS1 fraction was treated with antibody-linked magnetic beads (Dyna-beads), which are cross-linked with normal rabbit or mouse IgG, and then the beads were removed. It was confirmed that DJ-1 and synaptophysin were not lost under this condition (Fig. 4B). Pre-cleaned LS1 was incubated with the Dyna-beads cross-linked with the DJ-1 antibodies, and then the vesicle isolates containing DJ-1 were subjected to immunoblotting with the DJ-1 antibody. Interestingly, synaptophysin and VAMP2 also localized with the DJ-1-associated vesicles (Fig. 4C). HSP70, which is known as a nuclear and cytosolic protein (Daugaard et al., 2007), was not isolated by this procedure (Fig. 4C). This indicates that the synaptic vesicle fraction was not contaminated with the cytosolic fraction. Therefore, this suggests that DJ-1, synaptophysin, and VAMP2 might localize on the surface of the same vesicle. In addition, it was further investigated whether DJ-1 directly interacts with synaptophysin and/or VAMP2. The LS1 fraction treated with RIPA buffer was immunoprecipitated with pull-down beads cross-linked

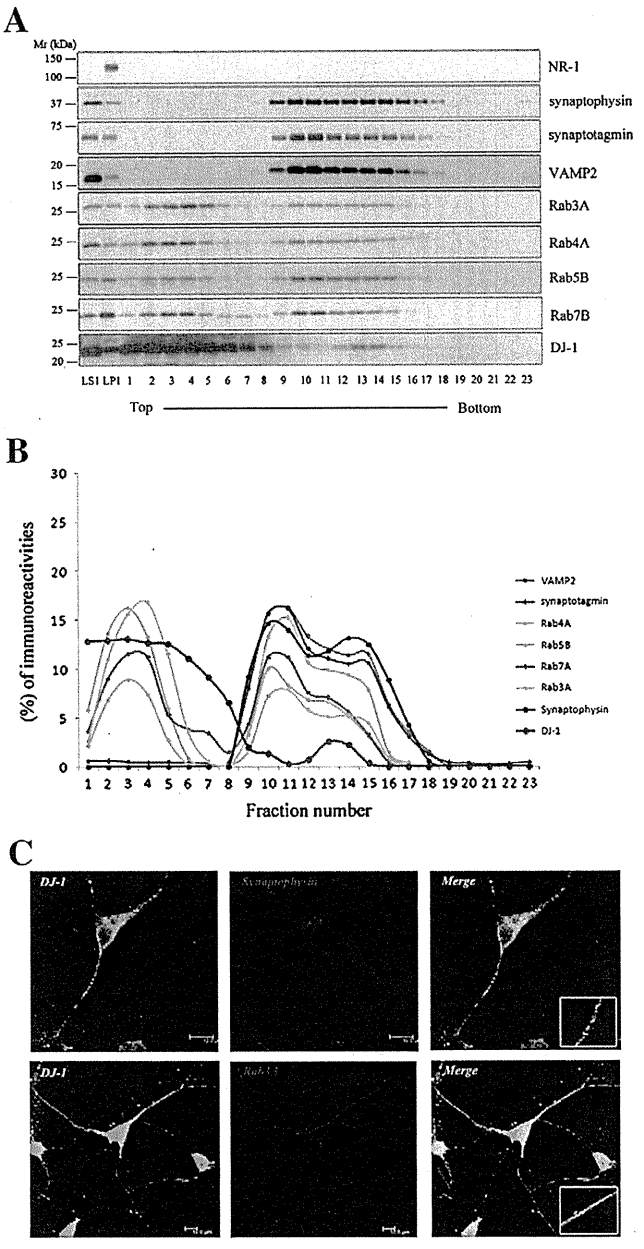

Fig. 3. DJ-1 associates with synaptic vesicles and colocalizes with synaptophysin and Rab3A. (A) The LS1 fraction was layered on top of a linear sucrose density gradient ranging from 0.2–2.0 M sucrose dissolved in HEPES buffer. Fractions were collected and 15 μl of each fraction were subjected to SDS–PAGE followed by immunoblotting using various markers. (B) Using the results from panel A, IR of each fraction was quantified and graphed as a percentage of each IR to the total immunoreactivities in each marker. DJ-1 had a biphasic profile of the immunoreactivities in fractions 1–8 and fractions 12–14, which indicated that there was some cytosolic fraction and some vesicle fractions. The peak of DJ-1 IR was in agreement with the latter peak of synaptophysin and Rab3A. (C) Primary cortical neurons from the mouse brain were fixed, permeabilized, and immunostained with DJ-1 antibody, and double-stained for synaptophysin and Rab3A. DJ-1 overlapped with synaptophysin and Rab3A. Scale bars = 10 μm.

with the synaptophysin antibody. It was found that VAMP2 interacts with synaptophysin as previous studies had reported (Baumert et al., 1989; Edelmann et al., 1995; Trimble et al., 1988). Immunoblotting with DJ-1 antibodies did not reveal endogenous DJ-1 in the resultant immunoprecipitates (Fig. 4C), whereas, endogenous synaptophysin and VAMP2 were not immunoprecipitated with the DJ-1 antibody.

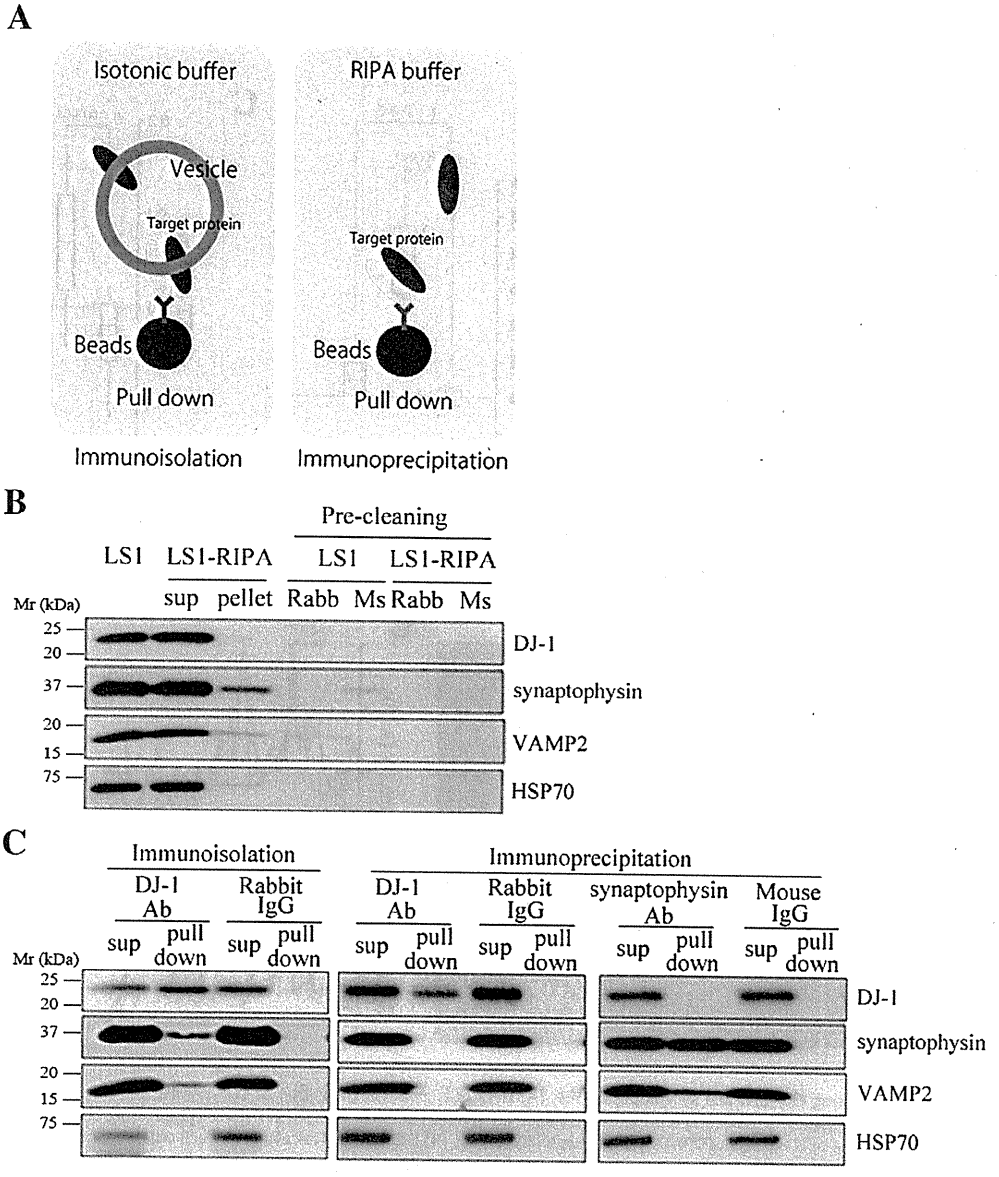

Fig. 4. DJ-1 cannot directly interact with synaptophysin and VAMP2, but associates with the same synaptic vesicles. (A) Image of immunoisolation and immunoprecipitation. Immunoisolation was used to pull down the target protein from the subcellular organelles (synaptic vesicle) from the homogenate, which was reacted with the isotonic buffer. Meanwhile, immunoprecipitation was used to pull down the target protein from the homogenate, which reacted with the buffer containing the detergent in order to examine the direct interactions between proteins. These methods were then used to assess the protein localized on the subcellular organelles with the target protein. (B) The LS1 fraction was first pre-cleaned. To remove nonspecifically-binding material, the LS1 fraction was treated with Dyna-beads cross-linked with normal rabbit or mouse IgG. It was confirmed that the targeting proteins were not lost in this reaction. (C) Sucrose buffer or RIPA buffer extracts of the mouse brain synaptic vesicle fractions were immunoisolated or immunoprecipitated using Dyna-beads coated with each antibody. Immunoisolates, immunoprecipitates and their corresponding supernatants were subjected to SDS–PAGE followed by immunoblotting using antibodies against the indicated proteins. Synaptophysin and VAMP2 were immunoisolated using Dyna-beads coated with the DJ-1 antibody, but they were not immunoprecipitated with the same bead slurry. Sup, supernatant.

Consequently, this proves that DJ-1 cannot directly interact with synaptophysin and VAMP2, but colocalizes with them on the same vesicles.

FRET analyses were performed to examine whether DJ-1 interacts with synaptophysin. We confirmed that FRET occurred between CFP–VAMP2, considered as positive control and synaptophysin-YFP (Pennuto et al., 2002). However, FRET was detected only in a small proportion of HeLa cells expressing CFP–DJ-1 and synaptophysin-YFP (Fig. 5A). $FRET_C$ median values with CFP–VAMP2, CFP–DJ-1, and CFP alone for more than 20 cells, were expressed as 0.363, 0.0413, and 0.0163, respectively (Fig. 5B). 293F cells expressing CFP–VAMP2 or CFP–DJ-1 and synaptophysin-YFP were also subjected to fluorescence lifetime flow cytometry, and fluorescence lifetimes of more than 10,000 cells in each sample were measured. Again, FRET efficiency observed between DJ-1 and synaptophysin was substantially lower than that between VAMP2 and synaptophysin, but significantly higher than that of the control (Fig. 5C). Confocal microscopic analyses revealed that CFP–DJ-1 also merged with synaptophysin-YFP. This pattern is similar to the colocalization between CFP–VAMP2 and synaptophysin-YFP (Fig. 5D, E). These results indicate that DJ-1 is able to localize with synaptophysin-positive vesicles and may interact with synaptophysin in living cells.

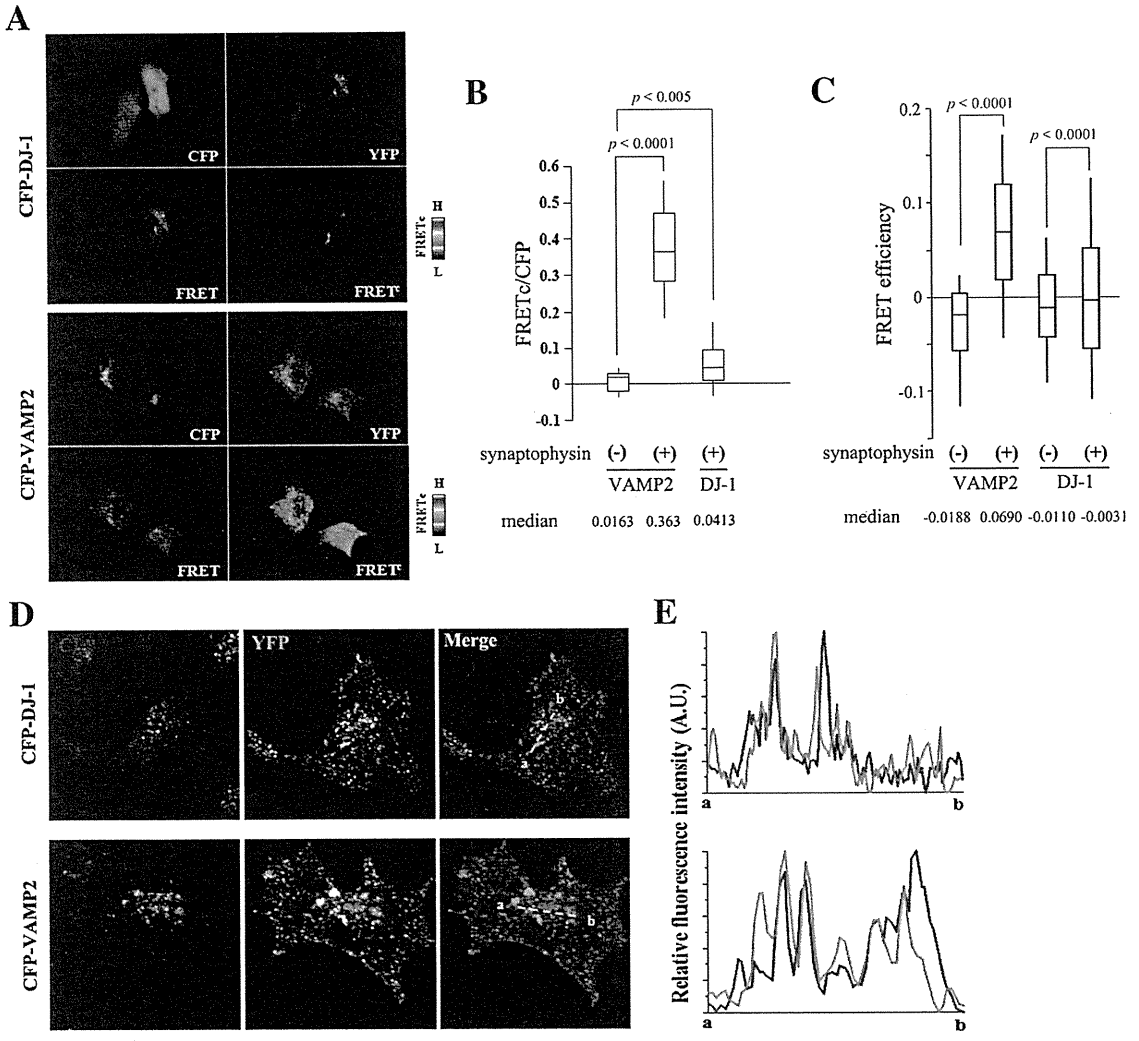

Fig. 5. FRET occurred in HeLa cells expressing CFP–DJ-1 and synaptophysin-YFP. (A) HeLa cells expressing CFP–DJ-1 or CFP–VAMP2, and synaptophysin-YFP were subjected to microscopic analysis as described in Materials and methods, and representative images are shown. FRET was detected in HeLa cells expressing CFP–VAMP2 and synaptophysin-YFP. FRET occurred in a small proportion of HeLa cells expressing CFP–DJ-1 and synaptophysin-YFP. (B) $FRET_C$ values calculated for each cells were plotted in the box and whisker plot. Representative data from three independent experiments are shown. The highest and lowest boundaries of the box represent the 25th and 75th percentiles, respectively, and whiskers above and below the box designate the 10th and 90th percentiles, respectively; the line within the box indicates the median value. (C) 293F cells expressing CFP–DJ-1 or CFP–VAMP2 and synaptophysin-YFP were subjected to fluorescence lifetime flow cytometry as described in Materials and methods. Fluorescence lifetimes of more than 10,000 cells in every sample were plotted in the box and whisker plot, where the highest and lowest boundaries of the box represent the 25th and 75th percentiles, respectively, and whiskers above and below the box designate the 10th and 90th percentiles, respectively; the line within the box indicates the median value. (D) Cells were imaged on a confocal laser microscope and representative images are shown. In a small proportion of cells CFP–DJ-1 merged with synaptophysin-YFP. CFP–VAMP2 colocalized with synaptophysin-YFP. (E) Fluorescence intensities of CFP (red) and YFP (green), along with the line in the merged image in (D), were plotted from a to b. Note that overlapping peaks indicate colocalization.

DJ-1 directly associates with membranes

The results from the immunocytochemical and biochemical experiments indicated that DJ-1 localizes in membranous structures, but it is unclear how DJ-1 associates with membranes. To address this issue, the effect of ionic strength on the association between DJ-1 with membranes was examined. PC12 cells were fractionated by centrifugation at 100,000g to pellets and supernatants, corresponding to membrane and cytosolic fractions, respectively. DJ-1 was collected in both the cytosol and the membranes. Although DJ-1 does not shift from the membrane to the cytosol regardless of high salt conditions, non-ionic detergent Triton X-100 solubilizes DJ-1 in a way similar to that of the transferrin receptor (Tfn-R) with a transmembrane domain (Fig. 6A). Meanwhile, parkin, which associates with lipid rafts (Fallon et al., 2002; Kubo et al., 2001), did not dissociate from the membrane by solubilization with Triton X-100 (Fig. 6A).

To characterize membrane-binding of DJ-1 protein, an in vitro binding assay using PC12 cells was employed as previously described (Kubo et al., 2005). In this assay, DJ-1 was found to be bound to purified plasma membranes. Treatment of plasma membranes purified from PC12 cells with Proteinase K (PK) for 60 min at 30 °C did not alter the localization of DJ-1 (Fig. 6C). We confirmed that digestion in PK for 60 min largely eliminated the protein as detected by silver staining (Fig. 6B).

L166P mutation affects membrane-binding ability

To investigate the pathogenicity of the mutant DJ-1 on membrane-binding ability, a membrane-binding assay was performed using the GST recombinant protein of wild type DJ-1 (GST–DJ-1 WT) and various pathogenic mutants. To eliminate the effects of endogenous DJ-1, DJ-1 knockout (KO) mice were used for this experiment. Synaptosomes from

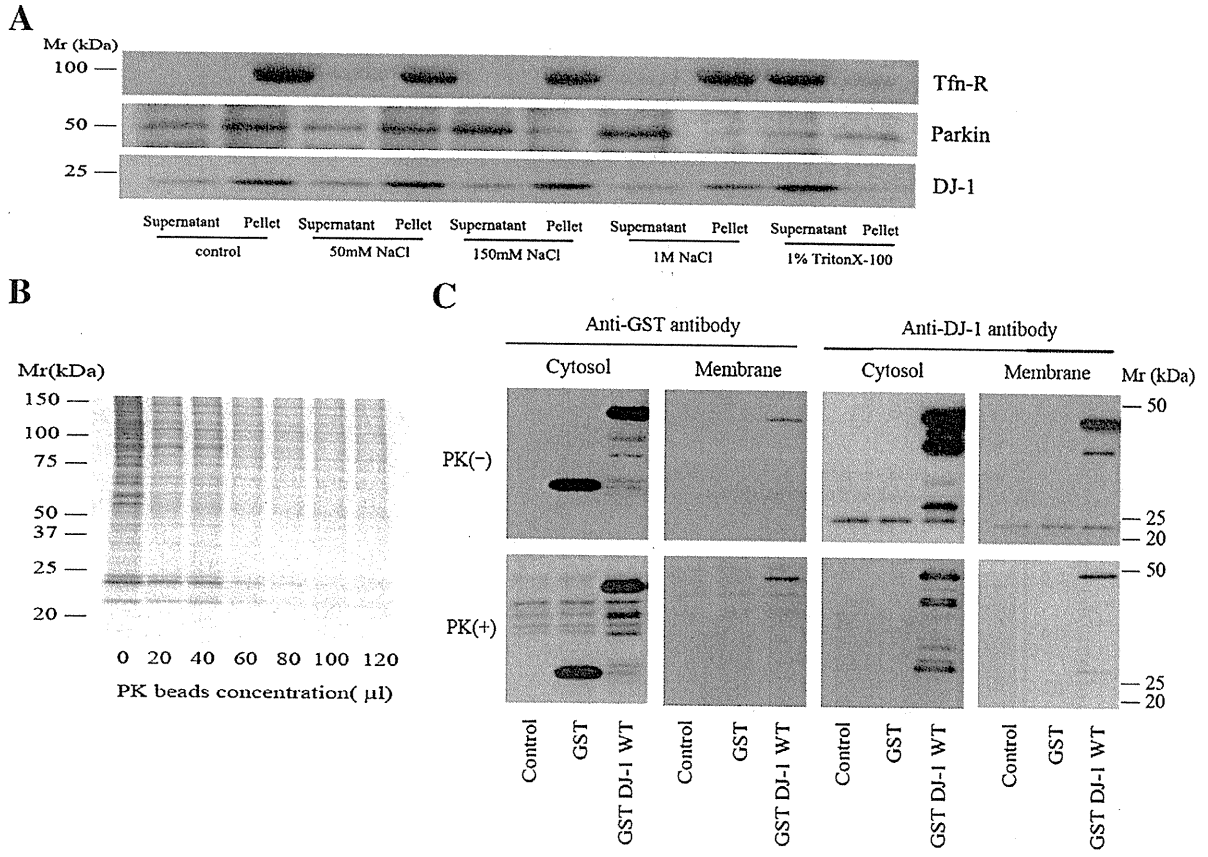

Fig. 6. Endogenous DJ-1 associates with cytosol and plasma membrane in PC12 cells. (A) Effects of various salt concentrations and non-ionic detergent on solubilization of DJ-1, Parkin, and transferrin receptor (Tfn-R). DJ-1 was concentrated in both the cytosol and membrane fractions of PC12 cells in the detergent-free isotonic buffer (control). DJ-1 did not shift from the membrane to the cytosol with increasing salt concentration, whereas Parkin relocalized from the membrane to cytosol, and Tfn-R remained in the pellet. However, DJ-1 did release from the membrane after being subjected to Triton X-100. Tfn-R was readily solubilized in this condition as well. Parkin remained in the pellet. Equal volumes of each of the fractions were loaded, followed by immunoblotting. (B) Silver staining of PC12 membranes treated with Proteinase K (PK) for 60 min at 30 °C showed a progressive loss of detectable membrane proteins with increasing PK concentration. (C) Recombinant DJ-1 wild type (WT), fused at its N terminus to the GST protein, was reacted with PC12 membranes or PK-treated membranes for 60 min at 30 °C. The GST-tagged protein, which served as a negative control, was also reacted. The reacted samples were centrifuged and divided into supernatant and pellet. Both supernatant and pellet were subjected to SDS–PAGE followed by immunoblotting. Anti-GST antibody detected the GST–DJ-1 WT recombinant protein band in the pellet fraction, whereas the GST-tagged protein was not detected in the pellet fraction. GST–DJ-1 WT recombinant protein directly associated with the plasma membrane in the in vitro assay.

DJ-1 KO mice were incubated with the GST–DJ-1 WT recombinant protein, or the GST–DJ-1 mutant recombinant proteins. Bound proteins were separated by centrifugation at 260,000g for 2 h. Compared with WT, the L166P mutant exhibited less binding to the synaptic membranes obtained from DJ-1 KO mice. However, there were no apparent differences between other pathogenic mutants and the WT in their membrane-binding property (Fig. 7A, B).

To further analyze the subcellular localization of various pathogenic DJ-1 mutants, HeLa cells were transfected with various DJ-1 mutants, as well as WT DJ-1 as control. M26I, A104T, and D149A showed diffuse and punctate distribution, similar to WT. By comparison, L166P exhibited localization near the plasma membrane (Fig. 7C).

Discussion

The overarching goal of this study was to determine the endogenous localization and membrane binding ability of DJ-1 and to elucidate potential differences in its properties between WT and pathogenic mutants. Immunocytochemistry for endogenous DJ-1 showed that the labeled structures distributed diffusely and displayed punctate staining. In the biochemical experiments, endogenous DJ-1 localized to the Golgi apparatus, cellular membranes, and synaptic vesicles which contain synaptophysin and Rab proteins. The GST–DJ-1 protein was found to be bound to cultured cellular membrane and mouse synaptosomes, as evidenced in the in vitro binding assay. Furthermore, this study shows that compared with WT, the L166P mutant exhibited less binding to the synaptic vesicles from DJ-1 KO mice.

Although several studies have reported on the mitochondrial localization of DJ-1 in cultured cells and mouse brains (Bonifati et al., 2003; Canet-Aviles et al., 2004; Miller et al., 2003; Zhang et al., 2005), Bandopadhyay et al. reported that they could not confirm the mitochondrial localization of endogenous DJ-1 in mouse primary astrocytes and hippocampal neurons (Bandopadhyay et al., 2004). Olzmann et al. described that DJ-1 localizes to the striatal axons and pre-synaptic terminals, suggesting a role for DJ-1 in dopaminergic neurotransmission (Olzmann et al., 2007). Zhang et al. also showed that DJ-1 was found in a synaptic-enriched fraction, however, they did not mention whether DJ-1 is associated with membrane trafficking (Zhang et al., 2005). In our experiments, DJ-1 partly localized to the synaptic cytosol, vesicles and membranes in the synaptic terminals of the mouse brain. However, a small portion of endogenous DJ-1 was located in mitochondria under steady state conditions, consistent with previous reports (Bandopadhyay et al., 2004; Nural et al., 2009). Thus, the present findings of endogenous DJ-1 localization provide evidence that DJ-1 may be associated with synaptic vesicles.

DJ-1 has the same distribution as members of the monomeric GTPases family called Rab proteins, known through biochemical

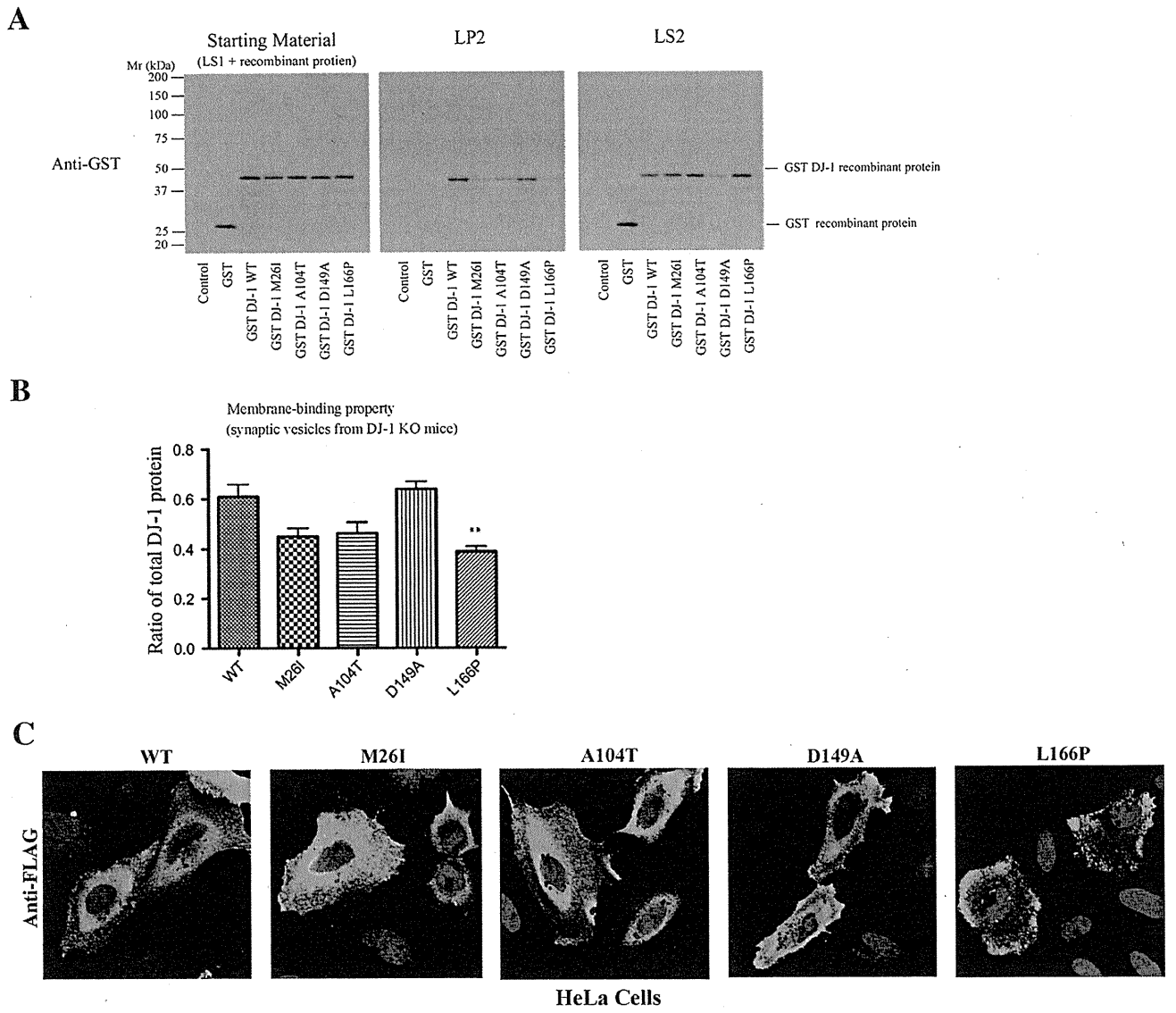

Fig. 7. Pathogenic DJ-1 mutants can bind membranes in the in vitro assay. (A) The LS1 fraction of DJ-1 KO mouse was reacted for 20 min at 30 °C with 500 nM GST recombinant protein, WT, or various mutants. Each of the bound proteins was divided into an LP2 fraction (synaptic vesicles) and an LS2 fraction (synaptic cytosol) by ultra-centrifugation at 260,000g for 2 h at 4 °C. The samples were subjected to SDS–PAGE followed by immunoblotting. The A104T, L166P, and M26I mutations also had lower bands corresponding to synaptic vesicles (LP2 fraction), compared with WT and D149A DJ-1. The GST-tagged protein, which served as a negative control was not detected. (B) Quantitative data from three independent experiments showed that the L166P mutant had reduced binding ability with the synaptic membrane. Immunoreactivity was quantified and expressed as percentage of bound (LP2) to total DJ-1 protein (LP2 + LS2). The data were plotted as the mean ± SEM. $^{**}P<0.001$ vs. WT, one-way ANOVA with Dunnett's Multiple Comparison Test. The other mutations were not statistically significant. The data were analyzed by GraphPad Prism (GraphPad Software, Inc.). (C) HeLa cells were transfected with expression vectors for FLAG-DJ-1 WT, M26I, A104T, D149A, or L166P. After 24 h, immunocytochemistry assay was performed on the cells. WT and the mutants, with the notable exception of the L166P mutant, appeared to have diffused subcellular distribution. WT was localized to the cytosol and in punctate spots. Similar results were obtained for mutants DJ-1, except for L166P. L166P localized near the plasma membrane.

studies as proteins associated with membrane trafficking (Harald Stenmark, 2001). DJ-1 may possibly associate with one and/or some of the Rab proteins. Actually, DJ-1 was found to partly colocalize with Rab3A by double-staining. Rab3A associates with immature secretory granules from the trans-Golgi network and has positive roles in exocytosis (Handley et al., 2007). Considering the colocalization between DJ-1 and Rab3A at synaptic terminals, DJ-1 could be involved in the vesicular trafficking system in such processes as exocytosis. Actually, DJ-1 KO mice exhibited altered synaptic functions, such as less sensitivity to the inhibitory effects of D2 auto receptor stimulation (Goldberg et al., 2005).

How can DJ-1 participate in synaptic vesicle transport? Corresponding with the results of the in vitro immunoisolation and immunoprecipitation assay, DJ-1 was found to not bind synaptophysin and VAMP2 directly, but DJ-1 localized with the synaptophysin and VAMP2-associated vesicles. In the in vivo FRET assay, a small portion of DJ-1 interacted with synaptophysin. Therefore, part of DJ-1 may be fairly close to synaptophysin and VAMP2. Neurotransmitter exocytosis involves sequential association of many synaptic proteins. Vesicular fusion, which is the central process of exocytosis, is mediated by the regulation of soluble N-ethylmaleimide sensitive factor (NSF) attachment protein receptor complexes, including VAMP2, syntaxin and synaptosome-associated protein 25 kDa (SNAP-25). These proteins interact with each other and play a critical role in the step between vesicle docking and fusion (Edelmann et al., 1995). Interestingly, several steps of vesicle fusion are regulated by molecular chaperones such as

NSF, 70 kDa heat-shock cognate protein, and cysteine-string protein (Zinsmaier and Bronk, 2001). DJ-1 is supposed to be a member of the DJ-1/YajL/PfpI superfamily, which function as molecular chaperones, and in RNA binding and hydrolase activity (Wei et al., 2007). Therefore, DJ-1 may participate in the regulation of neurotransmitter release as a molecular chaperone on synaptic vesicles.

From the results of the membrane-binding assay, DJ-1 was found to directly associate with membranes without an intermediary protein. Considering that the membrane binding of DJ-1 was not influenced by high-salt conditions, DJ-1 does not appear to associate with the membrane through electrostatic interactions such as ionic bonds, hydrogen bonds, and van der Waals attraction. Incubation with the non-ionic detergent Triton X resulted in release of DJ-1. This may mean that DJ-1 might prefer not to associate with lipid rafts, which are microdomains on membranes containing GM1 ganglioside, GPI anchor proteins, and several other membrane proteins (Edidin, 2003; Legler et al., 2005). Additionally, DJ-1 has no obvious amino acid sequences that serve as a targeting signal and transmembrane domains based on computer analysis (Kyte, 1982). Therefore, DJ-1 probably attaches to membranes through hydrophobic interactions.

Membrane proteins can bind to the lipid bilayer in various ways (Bruce Alberts, 2002; Lomize et al., 2007). In the proteins, peripheral membrane proteins temporarily adhere to the surface of the membrane. Some of them interact with membranes via an amphipathic α helix in the cytosolic monolayer (Bruce Alberts et al., 2002; Lomize et al., 2007). Based on crystal analyses, DJ-1 consists of a six-stranded parallel β-sheet sandwiched by eight α-helices and with a β-hairpin on one end and a three-stranded anti-parallel β-sheet on the opposite end (Anderson and Daggett, 2008; Wilson et al., 2003). Although the structure of DJ-1 is similar to that of a bacterial protein Pfp1, which is known as a cysteine protease, one major difference is the presence of an additional α-helix (helix αH) at the C terminus of DJ-1. The function of the helix αH is assumed to play a role in dimerization in combination with the helix αG (Honbou et al., 2003; Wilson et al., 2003). L166P is at the middle of the helix αG and is associated with significant structural deformations in this helix (Wilson et al., 2003). Additionally, the L166P mutant influences the membrane-binding property and disrupts the DJ-1 dimer (Anderson and Daggett, 2008). Therefore, we suspect that the α helices at the C terminus of DJ-1 are also able to function in membrane binding.

We also showed that the L166P mutant exhibits less binding to the synaptic vesicles from the DJ-1 KO mice compared with the WT, using the membrane-binding assay with the WT and various pathogenic mutations. Considering that the membrane-binding abilities of other mutations had no statistical difference with WT, it is presumed that the helix αG at the C terminus of DJ-1 associates with membrane binding. Actually, the results of the immunocytochemistry analysis of WT or mutants of DJ-1-overexpressing cells also revealed that the L166P mutant altered intracellular localization.

Based on our experiments, we believe that the association between DJ-1 and synaptic vesicles may contribute to the pathomechanisms in *PARK7*-linked PD. The previous studies have reported that α-synuclein, Parkin, and LRRK2 also localize to synaptic membranes and are associated with membrane trafficking (Abeliovich et al., 2000; Fallon et al., 2002; Hatano et al., 2007; Kahle et al., 2000; Kubo et al., 2001; Shin et al., 2008). Abnormality of membrane trafficking could be considered an important pathomechanism of PD as a common pathway. Further research may elucidate how DJ-1 associates with synaptic vesicles and why the loss of DJ-1 causes dopaminergic neuronal degeneration in PD.

Conclusions

This study is the first report showing the precise localization of endogenous DJ-1. We showed that DJ-1 colocalized with the Golgi apparatus proteins GM130 and the synaptic vesicle proteins synaptophysin and Rab3A. Although wild-type DJ-1 protein directly associated with membranes without an intermediary protein, the pathogenic L166P mutation of DJ-1 exhibited less binding to synaptic vesicles. Our findings indicate that DJ-1 associates with membranous organelles including synaptic membranes for its normal function.

Acknowledgments

We thank Norihiro Tada, Sachiko Ujiie, Sumihiro Kawajiri, Yuanzhe Li, Yoko Imamichi, and Akiko Egashira (Juntendo University). We are grateful to Shigeo Okabe and Shinji Tanaka (the Department of Cellular Neurobiology Graduate School of Medicine University of Tokyo) for providing synaptophysin-YFP and pCAGGS-CFP vectors. This work was supported by grants for Scientific Research Priority Areas (to N. H.), Scientific Research B (to N. H.), Scientific Research C (to S. K.), Young Scientists B (to T. H. and S. I.) from the Japanese Ministry of Education, Culture, Sports, Science and Technology of Core Research for Evolutional Science and Technology in the Japan Science and Technology (to N. H.), and the Research for the Future program of the Japan Society for the Promotion of Science, a Takeda Science Foundation (to S. K.).

References

Abeliovich, A., et al., 2000. Mice lacking alpha-synuclein display functional deficits in the nigrostriatal dopamine system. Neuron 25, 239–252.
Anderson, P.C., Daggett, V., 2008. Molecular basis for the structural instability of human DJ-1 induced by the L166P mutation associated with Parkinson's disease. Biochemistry 47, 9380–9393.
Bandopadhyay, R., et al., 2004. The expression of DJ-1 (PARK7) in normal human CNS and idiopathic Parkinson's disease. Brain 127, 420–430.
Baumert, M., et al., 1989. Synaptobrevin: an integral membrane protein of 18,000 daltons present in small synaptic vesicles of rat brain. EMBO J. 8, 379–384.
Bonifati, V., et al., 2003. Mutations in the DJ-1 gene associated with autosomal recessive early-onset parkinsonism. Science 299, 256–259.
Bruce Alberts, A.J., Julian, Lewis, Martin, Raff, Keith, Roberts, Peter, Walter (Eds.), 2002. Molecular Biology of the Cell, fourth edition. Garland Science, a member of the Taylor & Francis Group, New York.
Burre, J., et al., 2007. Immunoisolation and subfractionation of synaptic vesicle proteins. Anal. Biochem. 362, 172–181.
Canet-Aviles, R.M., et al., 2004. The Parkinson's disease protein DJ-1 is neuroprotective due to cysteine-sulfinic acid-driven mitochondrial localization. Proc. Natl. Acad. Sci. U.S.A. 101, 9103–9108.
Daugaard, M., et al., 2007. The heat shock protein 70 family: highly homologous proteins with overlapping and distinct functions. FEBS Lett. 581, 3702–3710.
Edelmann, L., et al., 1995. Synaptobrevin binding to synaptophysin: a potential mechanism for controlling the exocytotic fusion machine. EMBO J. 14, 224–231.
Edidin, M., 2003. The state of lipid rafts: from model membranes to cells. Annu. Rev. Biophys. Biomol. Struct. 32, 257–283.
Fallon, L., et al., 2002. Parkin and CASK/LIN-2 associate via a PDZ-mediated interaction and are co-localized in lipid rafts and postsynaptic densities in brain. J. Biol. Chem. 277, 486–491.
Fearnley, J.M., Lees, A.J., 1991. Ageing and Parkinson's disease: substantia nigra regional selectivity. Brain 114 (Pt 5), 2283–2301.
Goldberg, M.S., et al., 2005. Nigrostriatal dopaminergic deficits and hypokinesia caused by inactivation of the familial Parkinsonism-linked gene DJ-1. Neuron 45, 489–496.
Gordon, G.W., et al., 1998. Quantitative fluorescence resonance energy transfer measurements using fluorescence microscopy. Biophys. J. 74, 2702–2713.
Handley, M.T., et al., 2007. Differential dynamics of Rab3A and Rab27A on secretory granules. J. Cell Sci. 120, 973–984.
Harald Stenmark, V.M.O., 2001. The Rab GTPase family. Genome Biol. 2, 3007.1–3007.7.
Hatano, T., et al., 2007. Leucine-rich repeat kinase 2 associates with lipid rafts. Hum. Mol. Genet. 16, 678–690.
Hatano, T., et al., 2009. Pathogenesis of familial Parkinson's disease: new insights based on monogenic forms of Parkinson's disease. J. Neurochem. 111, 1075–1093.
Hell, J. W. a. J., R., 1998. Preparation of synaptic vesicles from mammalian brain. Celis, J.E. (Eds). San Diego.
Honbou, K., et al., 2003. The crystal structure of DJ-1, a protein related to male fertility and Parkinson's disease. J. Biol. Chem. 278, 31380–31384.
Kahle, P.J., et al., 2000. Subcellular localization of wild-type and Parkinson's disease-associated mutant alpha-synuclein in human and transgenic mouse brain. J. Neurosci. 20, 6365–6373.
Kim, R.H., et al., 2005. DJ-1, a novel regulator of the tumor suppressor PTEN. Cancer Cell 7, 263–273.
Kubo, S., et al., 2005. A combinatorial code for the interaction of alpha-synuclein with membranes. J. Biol. Chem. 280, 31664–31672.
Kubo, S., et al., 2001. Parkin is associated with cellular vesicles. J. Neurochem. 78, 42–54.
Kyte, J.a.D.,.R.F., 1982. A simple method for displaying the hydropathic character of a protein. J. Mol. Biol. 157, 105–132.

Lee, S.J., et al., 2003. Crystal structures of human DJ-1 and *Escherichia coli* Hsp31, which share an evolutionarily conserved domain. J. Biol. Chem. 278, 44552–44559.
Legler, D.F., et al., 2005. Differential insertion of GPI-anchored GFPs into lipid rafts of live cells. FASEB J. 19, 73–75.
Lomize, A.L., et al., 2007. The role of hydrophobic interactions in positioning of peripheral proteins in membranes. BMC Struct. Biol. 7, 44.
Miller, D.W., et al., 2003. L166P mutant DJ-1, causative for recessive Parkinson's disease, is degraded through the ubiquitin–proteasome system. J. Biol. Chem. 278, 36588–36595.
Morciano, M., et al., 2005. Immunoisolation of two synaptic vesicle pools from synaptosomes: a proteomics analysis. J. Neurochem. 95, 1732–1745.
Niki, T., et al., 2003. DJBP: a novel DJ-1-binding protein, negatively regulates the androgen receptor by recruiting histone deacetylase complex, and DJ-1 antagonizes this inhibition by abrogation of this complex. Mol. Cancer Res. 1, 247–261.
Nural, H., et al., 2009. Dissembled DJ-1 high molecular weight complex in cortex mitochondria from Parkinson's disease patients. Mol Neurodegener. 4, 23.
Olzmann, J.A., et al., 2007. Selective enrichment of DJ-1 protein in primate striatal neuronal processes: implications for Parkinson's disease. J. Comp. Neurol. 500, 585–599.
Pennuto, M., et al., 2002. Fluorescence resonance energy transfer detection of synaptophysin I and vesicle-associated membrane protein 2 interactions during exocytosis from single live synapses. Mol. Biol. Cell 13, 2706–2717.
Shin, N., et al., 2008. LRRK2 regulates synaptic vesicle endocytosis. Exp. Cell Res. 314, 2055–2065.
Shinbo, Y., et al., 2005. DJ-1 restores p53 transcription activity inhibited by Topors/p53BP3. Int. J. Oncol. 26, 641–648.
Taira, T., et al., 2004a. Co-localization with DJ-1 is essential for the androgen receptor to exert its transcription activity that has been impaired by androgen antagonists. Biol. Pharm. Bull. 27, 574–577.
Taira, T., et al., 2004b. DJ-1 has a role in antioxidative stress to prevent cell death. EMBO Rep. 5, 213–218.
Takahashi, K., et al., 2001. DJ-1 positively regulates the androgen receptor by impairing the binding of PIASx alpha to the receptor. J. Biol. Chem. 276, 37556–37563.
Trimble, W.S., et al., 1988. VAMP-1: a synaptic vesicle-associated integral membrane protein. Proc. Natl. Acad. Sci. U.S.A. 85, 4538–4542.
Wei, Y., et al., 2007. Identification of functional subclasses in the DJ-1 superfamily proteins. PLoS Comput. Biol. 3, e10.
Wilson, M.A., et al., 2003. The 1.1-A resolution crystal structure of DJ-1, the protein mutated in autosomal recessive early onset Parkinson's disease. Proc. Natl. Acad. Sci. U.S.A. 100, 9256–9261.
Yokota, T., et al., 2003. Down regulation of DJ-1 enhances cell death by oxidative stress, ER stress, and proteasome inhibition. Biochem. Biophys. Res. Commun. 312, 1342–1348.
Zhang, L., et al., 2005. Mitochondrial localization of the Parkinson's disease related protein DJ-1: implications for pathogenesis. Hum. Mol. Genet. 14, 2063–2073.
Zinsmaier, K.E., Bronk, P., 2001. Molecular chaperones and the regulation of neurotransmitter exocytosis. Biochem. Pharmacol. 62, 1–11.

SAGE-Hindawi Access to Research
Parkinson's Disease
Volume 2011, Article ID 473640, 5 pages
doi:10.4061/2011/473640

Clinical Study

Nonmotor Symptoms in Patients with *PARK2* Mutations

Asako Yoritaka,[1] Yumi Shimo,[1] Yasushi Shimo,[1] Yuichi Inoue,[2] Hiroyo Yoshino,[1] and Nobutaka Hattori[1]

[1] *Department of Neurology, Juntendo University School of Medicine, 2-1-1 Hongo, Bunkyo-ku, Tokyo 113-8421, Japan*
[2] *Japan Somnology Center, Neuropsychiatric Research Institute, 1-24-10 Yoyogi, Shibuya-ku, Tokyo 151-0053, Japan*

Correspondence should be addressed to Asako Yoritaka, ayori@juntendo.ac.jp

Received 14 October 2010; Accepted 16 December 2010

Academic Editor: Irena Rektorova

Decreased ^{123}I-meta-iodobenzylguanidine (MIBG) uptake in MIBG myocardial scintigraphy, olfactory dysfunction, and rapid eye movement (REM) sleep behavior disorder (RBD) are considered useful early indicators of Parkinson disease. We investigated whether patients with *PARK2* mutations exhibited myocardial sympathetic abnormalities using MIBG scintigraphy, olfactory dysfunction using the Sniffin' Sticks olfactory test, and RBD using polysomnography. None of the examined patients had RBD, and all except 1 patient exhibited an increase in the olfactory threshold. Moreover, one of the oldest patients exhibited impairment in identification and discrimination. Of 12 patients with *PARK2* mutations, 4 patients, who were older than patients without abnormal uptake, exhibited decreased MIBG uptake. The results obtained in this study suggest that some patients with *PARK2* mutations have increased thresholds of olfactory function and myocardial sympathetic dysfunction as nonmotor symptoms.

1. Introduction

Mutations in the *parkin* gene (*PARK2*) are considered to be the predominant cause of early-onset Parkinson disease particularly when the family history is compatible with autosomal recessive inheritance [1]. This condition is characterized by early onset of disease, usually before the age of 40 years, dystonia, sleep benefit, early complications from levodopa treatment, and slow progression. *Parkin*-associated tremor-dominant parkinsonism includes a spectrum of late-onset disorders without manifestations of foot dystonia, hyperreflexia, diurnal fluctuations, sleep benefit, or early susceptibility to levodopa-induced dyskinesia [2]. Therefore, patients with *PARK2* mutations are often clinically indistinguishable from those with sporadic Parkinson's disease (PD).

PD patients exhibit decreased myocardial uptake of meta-iodobenzylguanidine (MIBG) during ^{123}I-MIBG myocardial scintigraphy—a finding indicative of cardiac sympathetic denervation [3]. Olfactory impairment, an early symptom of PD, occurs in more than 70% of patients with PD [4]. Rapid eye movement (REM) sleep behavior disorder (RBD) is characterized by a loss of normal skeletal muscle atonia and complex motor activity, specifically during REM sleep associated with dream mentation. Thirty-eight percent of RBD patients aged ≥ 50 years were eventually diagnosed with PD [5]; therefore, RBD may serve as an early indicator of PD.

Here, we examined nonmotor symptoms in patients with *PARK2* mutations.

2. Methods

Mutation of the parkin gene was confirmed by gene analysis [1]. Eight women and 7 men possessed mutations in the *PARK2* gene: cases 1, 2, 3, 8, and 13 carried homozygous-deletions, and the remaining carried heterozygous mutations or deletions (Table 1). Clinical findings and medications are shown in Table 1.

The MIBG study involved 6 women and 7 men (mean (SD) age, 58.5 (11.4) years) with *PARK2* mutations: 5 subjects had homozygous deletions, and 8 had heterozygous mutations or deletions. Patients had parkinsonism for a mean (SD) period of 22.0 (11.59) years (range, 10–44 years). When MIBG scintigraphy was performed, the patients were not medicated with monoamine oxidase B (MAOB) inhibitors, selective serotonin reuptake inhibitors, or antidepressant drugs. Data was collected by E CAM at 30 minutes and 3 hours after injection of ^{123}I-MIBG

Table 1: Clinical findings and medication of patients with PARK2 mutation.

Case	1	2	3	4	5	6	7	8	9	10	11	12	13	14
Age sex	71 F	55 M	46 M	41 F	38 M	36 F	76 M	70 M	63 M	61 F	61 F	60 F	57 M	44 F
Parkin	exon 2–4 homo deletion	exon 5 homo deletion	exon 6, 7 homo deletion	exon 6 hetero deletion	exon 4, intron 4 accepter site, A → G	exon 10 hetero mutation	exon 10 hetero mutation	exon 2 homo-deletion	exon 2, 3, 4 hetero deletion	exon 2, 3 hetero deletion	exin 4 hetero deletion	exon 3, 4 hetero deletion	exon 2, 3, 4 homo-deletion	exon 5 hetero deletion
On set	61	28	28	27	18	20	65	45	33	29	47	16	45	34
Disease duration	10	27	18	14	20	16	11	28	36	34	14	44	12	10
Family history	–	+	+	–	–	+	+	–	–	+	–	+	+	+
Hoehn & Yahr stage on	2	2	2	1	1.5	2	2	3	3	3	3	3	1	1
Rigidity*	1	1	0	1	2	0	1	0	0	1	0	0	0	0
Tremor*	1	0	0	1	0	0	1	1	0	0	0	0	0	0
Hesitation*	0	1	1	0	0	2	0	1	1	2	2	1	0	0
Wearing-off	+	+	+	–	+	+	–	+	+	+	+	–	+	–
Dementia	–	–	–	–	–	+**	–	–	–	–	–	–	–	–
Hallucination	–	–	–	–	–	+	–	–	–	–	+	–	–	–
Sleep violent behavior	–	–	–	–	–	–	–	–	–	–	–	–	–	–
Constipation	+***	–	–	–	–	–	–	–	–	–	+	–	–	–
Levodopa	700 mg	600 mg	600 mg	300 mg	400 mg	300 mg	–	300 mg	500 mg	995 mg	800 mg	200 mg	450 mg	–
Agonist non-ergot	prami-pexole 1.5 mg	prami-pexole 4.5 mg	prami-pexole 3 mg	ropinirole 9 mg	prami-pexole 1.5 mg	ropinirole 12 mg	prami-pexole 4.5 mg	–	prami-pexole 0.75 mg	prami-pexole 1.5 mg	prami-pexole 2.25 mg	ropinirole 16 mg	–	pram-ipexole 1.5 mg
Agonist ergot	–	pergolide 2.25 mg	–	–	caber-goline 4 mg	–	–	–	–	–	–	–	caber-goline 2 mg	–
Selegiline	–	5 mg	–	–	10 mg	5 mg	–	–	–	–	5 mg	–	2.5 mg	–
Entacapone	–	400 mg	600 mg	–	300 mg	600 mg	–	–	400 mg	–	–	–	–	–
Trihexyphenidyl	–	–	–	–	3 mg	–	–	5 mg	–	–	–	–	–	–
Amantadine	300 mg	150 mg	300 mg	–	300 mg	–	–	–	150 mg	200 mg	100 mg	300 mg	–	–

DID: dopa induced dyskinesia.
*UPDRS mean score **Thalamotomy ***no medication.

(MyoMIBG-I 123 injection, 111 MBq; FUJIFILM RI Pharma Co. Ltd.). The cut-off ratio of the heart to mediastinum (H/M) uptake ratio of ^{123}I-MIBG in our hospital was set at 1.45.

The olfactory function and polysomnography (PSG) study involved 3 women and 3 men (mean (SD) age, 47.8 (13.2) years) with *PARK2* mutations (Table 1).

The mean olfactory function scores of the PD patients and 10 age-matched Japanese controls, who were evaluated for comparison with patients with *PARK2* mutations, were determined by the Sniffin' Sticks test. Mean age of the controls without neurological disease or dementia was 46.0 (15.3) years (range, 39–79 years). The PD patients (mean age, 69.6 (6.6) years; range, 60–89 years; not age matched to patients with *PARK2* mutations) fulfilled the UK Brain Bank criteria for possible or probable clinical PD, with Hoehn-Yahr stages II and III without dementia.

Olfactory testing was examined by following 3 components. Olfactory threshold and odor discrimination and identification were investigated in 3 separate substrates using standardized Sniffin' Sticks [6]. Sniffin' Sticks are commercially available felt-tip pens.

Odor Thresholds. The olfactory threshold subset consisted of 16 Sniffin' Stick triplets with different concentrations of *n*-butanol. Three sticks were presented to the subject in randomized order. Two contained only the solvent and the third the odorant at a particular dilution. The subjects were tasked to identify the stick with the odorant.

Odor Discrimination. In the odor discrimination subset, 16 Sniffin' Stick triplets were presented in randomized order. Two pens contained the same odorant and the third a different odorant. The task was to identify the stick that had the different smell.

Odor Identification. The third subtest consisted of 16 single sticks and assessed the ability to identify an odor. Using a multiple-choice task, identification of individual odorants was performed from a list of 4 descriptors.

RBD was confirmed by studying the patients' clinical history and video-PSG findings (International Classification of Sleep Disorders, 2nd edition) [7].

Informed consent was obtained from patients with *PARK2* mutations, and patients with PD, and normal volunteers.

The data was statistically analyzed using SPSS ver.11 for Windows.

3. Results

The mean H/M uptake ratio of ^{123}I-MIBG scintigraphy in *PARK2* patients was 1.79 (0.31) in the early phase and 1.75 (0.51) in the delayed phase (Table 2). However, a 58-year-old woman, with a 10-year disease duration and orthostatic hypotension and constipation without myocardial damage, exhibited accelerated MIBG elimination (H/M ratio: early, 1.23; delayed, 1.15). Three patients (cases 2, 7, and 12) had exhibited slightly decreased uptake in the delayed phase.

The Sniffin' Sticks test revealed a slight olfactory dysfunction with the following mean scores in examined *PARK2* patients (Table 3): threshold score, 6.1 (1.6) ($P < .05$ when compared with controls); odor discrimination score, 10.0 (2.4); odor identification score, 10.1 (4.8) (no significant differences when compared to controls). Odor discrimination and identification functions were not impaired in any of the patients with *PARK2* mutations, except in patient 1. In the Japanese examined normative controls, the mean olfactory function scores were as follows: threshold score, 8.0 (1.3); discrimination score, 11.9 (2.4); identification score, 10.9 (2.0); in PD patients, these mean scores were 2.2 (6.6), 6.1 (2.5), and 5.1 (1.8), respectively.

PSG did not reveal tonic responses in the mentalis and tibialis muscles during REM (Table 3). Twitching of the tibialis muscle was observed in 2 patients. None of the patients with *PARK2* mutations met the ICSD-II criteria for RBD.

4. Discussion

Decreased ^{123}I-MIBG uptake was observed clearly in 1 patient with *PARK2* mutations who had autonomic dysfunction. Early phase myocardial uptake of MIBG in all of the other patients showed no decrease, and patients had no autonomic dysfunction. Similar to our study, in a previous study [8], 1 of 4 patients with *PARK2* mutations with a 12-year disease duration and unclear autonomic dysfunction exhibited decreased uptake of ^{123}I-MIBG. Additionally, 3 patients in our study who showed decreased ^{123}I-MIBG uptake were slightly older than the other patients, although a significance in mean age (63.0 (9.1) versus 55.9 (10.8); $P > .05$) did not exist. Estorch et al. and Tsuchimochi et al. reported that the uptake of ^{123}I-MIBG decreased with age, suggesting that aging could affect patients with *PARK2* mutations [9, 10]. Decreased myocardial uptake of MIBG is considered to indicate the presence of alpha-synuclein aggregates in the axons in PD [11]. In MIBG-myocardial scintigraphy, the H/M ratio of patients with *PARK2* mutations was reported to be within the range of the normal controls [12]. Moreover, postmortem examination of patients with *PARK2* mutations revealed that tyrosine hydroxylase immunoreactive nerve fibers in the epicardium were well preserved [13]. These findings might reflect normal functioning myocardial sympathetic nerve terminals in patients with *PARK2* mutations. MIBG scintigraphy might be a marker for alpha-synuclein in patients with *PARK2* mutations; however, there are no pathological reports on the presence of Lewy bodies in patients with *PARK2* mutations exhibiting decreased MIBG uptake.

Olfactory impairment is a nonmotor symptom of PD. We found that the olfactory threshold was slightly higher in patients with *PARK2* mutations than in controls. The oldest woman in our study, who did not have dementia, exhibited the highest degree of olfactory impairment. Although in self-completed questionnaire study, 3 of 16 patients with *PARK2* mutation had loss of taste/smell [14]. However, in previous

Table 2: The findings of ^{123}IMIBG myocardial scintigraphy in PARK2 patients.

Case	1	2	3	5	7	8	9	10	11	12	13	14	Average ± SD
Examined age	65	55	46	41	76	70	63	61	61	60	57	44	58.3 ± 10.5
Early H/M	2.27	1.64	1.91	1.75	1.52	2.05	1.75	1.66	1.23	1.75	1.62	2.35	1.79 ± 0.31
Delay H/M	2.14	1.33	1.67	1.93	1.34	2.93	1.65	1.54	1.15	1.40	1.60	2.35	1.75 ± 0.51

H/M: the heart to mediastinum uptake ratio of ^{123}IMIBG.

Table 3: Olfactory function by Sniffin' sticks and PSG study in patients with PARK2 mutation, controls, and Parkinson's disease.

Case	1	2	3	4	5	6	*PARK2* total ($n = 6$)	Control ($n = 10$)	Parkinson's disease ($n = 15$)
Age	71	55	46	41	38	36	47.8 ± 13.2	46.0 ± 15.3	69.6 ± 6.6
Sniffin' sticks Test									
Threshold test	4.5	6.3	6.3	5.8	5.0	9.0	6.1 ± 1.6	8.0 ± 1.3*	2.2 ± 2.3**
Discrimination test	8.0	9.0	12.0	14.0	9.0	8.0	10.0 ± 2.4	11.9 ± 2.4	6.1 ± 2.5
Identification test	1.0	13.0	10.0	14.0	13.0	10.0	10.1 ± 4.8	10.9 ± 2.0	5.1 ± 1.8
PSG findings									
Apnea index (times/H)	10.1	22.5	1.2	0.4	1.0	2.1			
Hypopnea index (times/H)	2.2	14.0	4.7	0.3	1.9	9.4			
Apnea Hypopnea index (times/H)	12.3	36.5	5.9	0.8	3.0	11.4			
Arousal index (times/H)	16.0	39.8	37.7	13.4	14.3	11.1			
Respiratory arousal index (times/H)	5.5	27.3	4.6	0.2	1.6	3.3			
PLM index(times/H)	7.8	0.0	7.7	0.0	29.5	0.0			
PLM arousal index(times/H)	0.0	0.0	5.3	0.0	2.8	0.0			
REM sleep twitching on TA muscle	−	+	−	+	−	−			

H/M: theheart to mediastinum uptake ratio, NE: not examined.
PLM: periodic limb movements, TA: tibialis anterior.
*t-test: compared with *PARK2* patients $P < .05$.
**t-test: compared with *PARK2* patients and control $P < .01$.

studies, individuals with *PARK2* mutations were found to have normal olfactory function [15, 16]. The discrepancy between our results and previous ones may be because previous studies used the Pennsylvania Smell Identification Test, which does not include the threshold test. In Kahn's study [15], the odor identification score did not significantly differ between patients with *PARK2* mutations and controls, although this did not necessarily imply that the threshold score was normal in the patients.

PSG did not reveal RBD in any of our patients. However, in a study by Kumru et al., 6 of 10 patients had RBD [17]. We cannot explain this discrepancy, but we hypothesize that it may be due to the differences in patient mean age between the 2 studies. Some of our patients with *PARK2* mutations have twitching in the tibialis muscle; therefore, the possibility that they will eventually develop RBD cannot be ruled out. Neuropathological studies on patients with *PARK2* mutations have revealed neuronal loss and gliosis in the pars compacta of the substantia nigra and in the locus coeruleus [18]. However, these studies have not described the state of the subcoeruleus nucleus, which is considered the primary site affected in RBD.

The results obtained in this study suggest that some patients with *PARK2* mutations have increased thresholds of olfactory function and myocardial sympathetic dysfunction as nonmotor symptoms. We might show that the nonmotor symptoms of *PARK2* were impaired heterogeneously.

Author Contributions'

A. Yoritaka was responsible for conception, execution of research projects, statistical analysis, writing of first draft and review and critique; Yasushi Shimo was responsible for execution of research project; Yumi Shimo and Y. Inoue were responsible for execution of research project (PSG study); H. Yoshino was responsible for gene analysis; N. Hattori was responsible for conception and organization of research project.

References

[1] T. Kitada, S. Asakawa, N. Hattori et al., "Mutations in the parkin gene cause autosomal recessive juvenile parkinsonism," *Nature*, vol. 392, no. 6676, pp. 605–608, 1998.

[2] M. M. Mouradian, "Recent advances in the genetics and pathogenesis of Parkinson disease," *Neurology*, vol. 58, no. 2, pp. 179–185, 2002.

[3] S. Orimo, E. Ozawa, S. Nakade, T. Sugimoto, and H. Mizusawa, "^{123}I-metaiodobenzylguanidine myocardial scintigraphy in Parkinson's disease," *Journal of Neurology Neurosurgery and Psychiatry*, vol. 67, no. 2, pp. 189–194, 1999.

[4] C. H. Hawkes, B. C. Shephard, and S. E. Daniel, "Olfactory dysfunction in Parkinson's disease," *Journal of Neurology Neurosurgery and Psychiatry*, vol. 62, no. 5, pp. 436–446, 1997.

[5] C. H. Schenck, S. R. Bundlie, and M. W. Mahowald, "Delayed emergence of a parkinsonian disorder in 38% of 29 older, men initially diagnosed with idiopathic rapid eye movement sleep behavior disorder," *Neurology*, vol. 46, no. 2, pp. 388–393, 1996.

[6] T. Hummel, B. Sekinger, S. R. Wolf, E. Pauli, and G. Kobal, "'Sniffin' sticks'. Olfactory performance assessed by the combined testing of odor identification, odor discrimination and olfactory threshold," *Chemical Senses*, vol. 22, no. 1, pp. 39–52, 1997.

[7] American Academy of Sleep Medicine, *International Classification of Sleep Disorders: Diagnostic and Coding Manual*, American Academy of Sleep Medicine, Westchester, Ill, USA, 2nd edition, 2005.

[8] A. Quattrone, A. Bagnato, G. Annesi et al., "Myocardial ^{123}metaiodobenzylguanidine uptake in genetic Parkinson's disease," *Movement Disorders*, vol. 23, no. 1, pp. 21–27, 2008.

[9] M. Estorch, I. Carrió, L. Berná, J. López-Pousa, and G. Torres, "Myocardial iodine-labeled metaiodobenzylguanidine 123 uptake relates to age," *Journal of Nuclear Cardiology*, vol. 2, no. 2, pp. 126–132, 1995.

[10] S. Tsuchimochi, N. Tamaki, S. Shirakawa et al., "Evaluation of myocardial distribution of iodine-123 labeled metaiodobenzylguanidine (^{123}I-MIBG) in normal subjects," *Kakuigaku*, vol. 31, no. 3, pp. 257–264, 1994.

[11] S. Orimo, T. Uchihara, A. Nakamura et al., "Axonal α-synuclein aggregates herald centripetal degeneration of cardiac sympathetic nerve in Parkinson's disease," *Brain*, vol. 131, no. 3, pp. 642–650, 2008.

[12] M. Suzuki, N. Hattori, S. Orimo et al., "Preserved myocardial [^{123}I] metaiodobenzylguanidine uptake in autosomal recessive juvenile parkinsonism: first case report," *Movement Disorders*, vol. 20, no. 5, pp. 634–636, 2005.

[13] S. Orimo, T. Amino, M. Yokochi et al., "Preserved cardiac sympathetic nerve accounts for normal cardiac uptake of MIBG in PARK2," *Movement Disorders*, vol. 20, no. 10, pp. 1350–1353, 2005.

[14] G. Kägi, C. Klein, N. W. Wood et al., "Nonmotor symptoms in Parkin gene-related parkinsonism," *Movement Disorders*, vol. 25, no. 9, pp. 1279–1284, 2010.

[15] N. L. Khan, R. Katzenschlager, H. Watt et al., "Olfaction differentiates parkin disease from early-onset parkinsonism and Parkinson disease," *Neurology*, vol. 62, no. 7, pp. 1224–1226, 2004.

[16] D. Verbaan, S. Boesveldt, S. M. van Rooden et al., "Is olfactory impairment in Parkinson disease related to phenotypic or genotypic characteristics?" *Neurology*, vol. 71, no. 23, pp. 1877–1882, 2008.

[17] H. Kumru, J. Santamaria, E. Tolosa et al., "Rapid eye movement sleep behavior disorder in parkinsonism with PARKIN mutations," *Annals of Neurology*, vol. 56, no. 4, pp. 599–603, 2004.

[18] H. Mori, T. Kondo, M. Yokochi et al., "Pathologic and biochemical studies of juvenile parkinsonism linked to chromosome 6q," *Neurology*, vol. 51, no. 3, pp. 890–892, 1998.

Role of the External Oblique Muscle in Upper Camptocormia for Patients with Parkinson's Disease

Patients with Parkinson's disease (PD) often experience camptocormia, a postural disorder with unclear pathophysiology and unestablished treatments.[1] We clinically categorized camptocormia as upper and lower types based on the location of inflection points. We defined upper camptocormia as abnormal truncal flexion at a point between the lower thoracic and upper lumbar vertebrae whose flexion angle exceeded 40 degrees, whereas lower camptocormia was defined as abnormal truncal flexion at the hip joint. This study focused on upper camptocormia.

We performed lidocaine injections into the abdominal muscles of PD patients with upper camptocormia and evaluated their effects on posture to investigate its pathophysiology. Patients with fixed posture because of spinal disease or truncal muscle weakness were excluded. We included 5 patients (4 women and 1 man; mean age, 70.8 ± 4.4 years; PD duration, 8.2 ± 3.9 years; Hoehn & Yahr stage, 2.6 ± 0.8) treated with antiparkinson drugs in our hospital. Camptocormia did not respond to these drugs in any of the patients. Ultrasound guidance was used for lidocaine injections into the abdominal muscle (rectus abdomen [RA] and external oblique [EO] in all patients; internal oblique [IO] in 2 patients; 50 mg in each muscle bilaterally). Although the order of each injection was different in each patient, the following injection was performed on confirming that improvement diminished or if no improvement was observed after several days. Flexion angles were measured before and after each injection. The angle formed between a line perpendicular to the ground and a line linking the C7 vertebra with the inflection point of the trunk was defined as the flexion angle. This study was approved by the NCNP ethics committee. Informed consent was obtained from all patients.

The posture of all patients improved following injection into the EO. The average flexion angle decreased from 49 ± 6.0 degrees to 37 ± 10 degrees (truncal angle of age-matched PD patients without camptocormia was 29.4 ± 3.7 degrees; Fig. 1), Only 1 patient showed mild improvement after injection into the RA. No improvements were observed following injection into the IO.

The RA performs truncal anteflexion, whereas the EO and IO work bilaterally for truncal flexion. Azher et al previously reported improvement of camptocormia by botulinum toxin injection into the RA,[2] although they did not classify camptocormia by type. In the present study, forward flexion was reduced in all patients after injection into the EO, not RA nor IO. Our results may suggest that the EO is primarily associated with upper camptocormia pathogenesis. Considering that previous studies have speculated that lidocaine could suppress dystonic excitation,[3–5] dystonia of the EO may be a cause of upper camptocormia.

Although this study has some limitations, such as the small number of patients and not adjusting lidocaine dose for muscle size, this is the first report to investigate camptocormia pathophysiology by classification, and these findings may contribute to the treatment of upper camptocormia in patients with PD. To confirm our results, we have been carrying out a larger study.

Acknowledgment: We express our deepest gratitude to Dr. Atsuo Nakagawa, whose extensive support and insightful comments were invaluable during the course of our study.

Yoshihiko Furusawa, MD[1]*, Yohei Mukai, MD[1], Yoko Kobayashi, PhD[2], Takashi Sakamoto, MD[1], Miho Murata, PhD[1]

[1]Department of Neurology, National Center Hospital of Neurology and Psychiatry Kodaira, Tokyo, Japan; [2]Department of Rehabilitation, National Center Hospital of Neurology and Psychiatry Kodaira, Tokyo, Japan

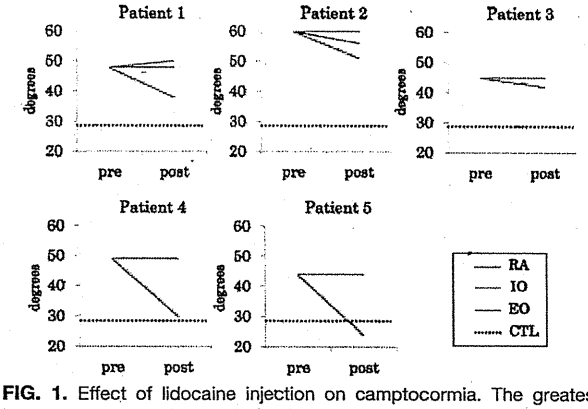

FIG. 1. Effect of lidocaine injection on camptocormia. The greatest improvement was observed after injection into the EO. The dotted line indicates the average truncal angle of control patients (RA, rectus abdomen; IO, internal oblique; EO, external oblique; CTL, control patients).

* **Correspondence to:** Yoshihiko Furusawa, Department of Neurology, National Center Hospital of Neurology and Psychiatry Kodaira, Tokyo, Japan; yfuru@ncnp.go.jp

Funding agencies: This work was supported in part by Grants-in-Aid from the Research Committee of CNS Degenerative Disease, the Ministry of Health, Labour and Welfare of Japan, and Intramural Research Grant (21B-4) for Neurological and Psychiatric Disorders of NCNP.

Relevant conflicts of interest/financial disclosures: Nothing to report. Full financial disclosures and author roles may be found in the online version of this article.

Published online in Wiley Online Library (wileyonlinelibrary.com). DOI: 10.1002/mds.24930

References

1. Melamed E, Djaldetti R. Camptocormia in Parkinson's disease. J Neurol 2006;253:VII14–VII16.
2. Azher SN, Jankovic J. Camptocormia: pathogenesis, classification, and response to therapy. Neurology 2005;65:355–359.
3. Kaji R, Rothwell JC, Katayama M, et al. Tonic vibration reflex and muscle afferent block in writer's cramp. Ann Neurol 1995;38:155–162.
4. Irwin D, Revuelta G, Lippa CF. Clinical improvement of secondary focal limb dystonia in neurodegenerative disease following a five-day lidocaine infusion: a case report. J Neurol Sci 2009;277:164–166.
5. Yoshida K, Kaji R, Kubori T, Kohara N, Iizuka T, Kimura J. Muscle afferent block for the treatment of oromandibular dystonia. Mov Disord 1998;13:699–705.

J Inherit Metab Dis (2012) 35:301–310
DOI 10.1007/s10545-011-9393-6

ORIGINAL ARTICLE

Effects of enzyme replacement therapy on five patients with advanced late-onset glycogen storage disease type II: a 2-year follow-up study

Yoshihiko Furusawa · Madoka Mori-Yoshimura · Toshiyuki Yamamoto · Chikako Sakamoto · Mizuki Wakita · Yoko Kobayashi · Yutaka Fukumoto · Yasushi Oya · Tokiko Fukuda · Hideo Sugie · Yukiko K. Hayashi · Ichizo Nishino · Ikuya Nonaka · Miho Murata

Received: 26 April 2011 / Revised: 4 September 2011 / Accepted: 8 September 2011 / Published online: 7 October 2011

Abstract We examined the efficacy of 2-year enzyme replacement therapy (ERT) using recombinant human α-glucosidase (GAA; Myozyme®) in five long-term ventilator-dependent adults and aged patients with advanced, late-onset glycogen storage disease type II (GSDII, also known as Pompe disease). Although all patients had advanced respiratory failure and were ventilator-dependent for more than 6 years, four showed obvious improvements in muscle strength, pulmonary function, and activities of daily living after ERT. Improvement in each parameter was more prominent in the first year than in the second year. Values in the second year were still significantly better than those at study entry and indicate stabilization in the clinical status of all patients. These results suggest that ERT continues to be effective in the second year of treatment even in patients suffering from advanced late-onset GSDII disease with severe respiratory failure.

Introduction

Glycogen storage disease type II (GSDII), or Pompe disease, is an autosomal recessive lysosomal glycogen storage disease

Communicated by: Ed Wraith

Competing interests: None declared.

Electronic supplementary material The online version of this article (doi:10.1007/s10545-011-9393-6) contains supplementary material, which is available to authorized users.

Y. Furusawa · M. Mori-Yoshimura (✉) · T. Yamamoto · Y. Oya · M. Murata
Department of Neurology, National Center Hospital, National Center of Neurology and Psychiatry, 4-1-1 Ogawahigashi-cho, Kodaira, Tokyo 187-8551, Japan
e-mail: yoshimur@ncnp.go.jp

C. Sakamoto · M. Wakita · Y. Kobayashi
Department of Rehabilitation, National Center Hospital, National Center of Neurology and Psychiatry, 4-1-1 Ogawahigashi-cho, Kodaira, Tokyo 187-8551, Japan

Y. Fukumoto
Dental Branch, National Center Hospital, National Center of Neurology and Psychiatry, 4-1-1 Ogawahigashi-cho, Kodaira, Tokyo 187-8551, Japan

I. Nonaka
Department of Child Neurology, National Center Hospital, National Center of Neurology and Psychiatry, 4-1-1 Ogawahigashi-cho, Kodaira, Tokyo 187-8551, Japan

T. Fukuda · H. Sugie
Department of Pediatrics, Jichi Medical School, 3311-1, Yakushiji, Shimotsuke-city, Tochigi 329-0498, Japan

Y. K. Hayashi · I. Nishino
Department of Neuromuscular Research, National Institute of Neuroscience, National Center of Neurology and Psychiatry, 4-1-1 Ogawahigashi-cho, Kodaira, Tokyo 187-8502, Japan

resulting from a deficiency in α-glucosidase (GAA) activity (OMIM #232300). The different clinical phenotypes of GSDII include classic infantile-onset; non-classic infantile-onset; childhood, juvenile, and adult forms of GSDII; and late-onset GSDII. However, GSDII presents as a broad spectrum with varying degrees of severity and rates of progression. The classic infantile-onset form is characterized by hypertrophic cardiomyopathy and generalized muscle weakness, which appear in the first few months of life (Hirshhorn and Reuser 2001; Engel et al. 2004). Late-onset GSDII is characterized by progressive skeletal muscle weakness and loss of respiratory function.

Enzyme replacement therapy (ERT) using recombinant human GAA (rhGAA) derived from transfected Chinese hamster ovary cells resulted in marked improvement in the survival rate of 18 patients with infantile-onset GSDII (Kishnani et al. 2008). Nicolino and colleagues also reported that rhGAA reduced the risk of death and invasive ventilation by 79 and 58%, respectively, in infants and children with advanced Pompe disease (Nicolino et al. 2009). The use of ERT with Myozyme® (α-glucosidase) was approved by the U.S. Food and Drug Administration (FDA) in 2006 and by the Japan Ministry of Health, Labor and Welfare (MHLW) in 2007.

Previous studies confirmed the efficacy of ERT in late-onset GSDII patients with acute respiratory failure or relatively mild respiratory dysfunction (Winkel et al. 2004; Pascual-Pascual et al. 2006; Merk et al. 2007, 2009; Case et al. 2008; Yamamoto et al. 2008; Rossi et al. 2007; van Capelle et al. 2008; Strothotte et al. 2010; van der Ploeg et al. 2010). On the other hand, ERT efficacy in advanced patients seemed to be lower than that in milder patients (Orlikowski et al. 2011). It is not clear whether ERT is continuously effective in ventilator-dependent patients with advanced disease and long-term respiratory failure. Because ERT is relatively expensive, it is important to determine whether continuous administration is effective, or whether therapy is only effective for a short duration. In the present study, we evaluated the efficacy of ERT in five patients with advanced late-onset GSDII for 2 years and analyzed factors related to its efficacy.

Patients and methods

Patients

Patients with late-onset Pompe disease diagnosed based on both muscle biopsies and fibroblast/muscle residual GAA activity, and who had undergone ERT at the National Center Hospital (National Center of Neurology and Psychiatry), were included in this study. Written informed consent was obtained before enrollment. The study protocol was approved by the National Center Hospital Ethics Committee. Patients 4 and 5 have been reported previously (Sasaki et al. 1992; Yamazaki et al. 1992). Table 1 lists the characteristics of all five patients (two men and three women).

Genomic DNA was extracted from blood or muscle biopsy samples according to standard protocols. All exons and flanking intronic regions of GAA were amplified and sequenced using an automated 3100 DNA sequencer (Applied Biosystems, Foster, CA). Primer sequences are available upon request. All patients had previously reported mutations (Tsujino et al. 2000; Tsunoda et al. 1996; Lam et al. 2003; Pipo et al. 2003; Hermans et al. 2004). The average (SD) age at ERT initiation was 47 (13.6) years (range 32–66 years), and the average duration of disease was 26 (4.5) years (range 20–31 years). The average duration of mechanical ventilatory support before ERT was 8.0 (1.9) years (range 6–11 years). Patients 1, 2, 4, and 5 had been treated with noninvasive ventilation (NIV), and patient 3 had been treated with invasive ventilation. All patients were wheelchair-bound for a mean of 7.0 (5.1) years (range 2–14 years). Only patient 4 was able stand for a few minutes or walk a few steps with assistance. Others were completely wheelchair-bound.

Methods

ERT (Myozyme®) was administered at 20 mg/kg body weight biweekly at a dose of 1 mg/kg/h for the first 30 min, 3 mg/kg/h for the second 30 min, and then increased to 5 mg/kg/h, and finally 7 mg/kg/h every 30 min. Patients were carefully monitored for infusion-related reactions during and after ERT administration. Clinical condition was assessed every 6 months, including physical examination, manual muscle test (MMT), ECG, Holter ECG, ultrasound cardiography (UCG), and pulmonary function tests [% vital capacity (%VC), % force vital capacity (% FVC), forced expiratory volume in the first second (FEV1.0), peak expiratory flow rate (PEF), peak cough flow (PCF; Bach 2004)], and lean body mass (Discovery Bone Densitometer, Hologic, Bedford, MA). Muscle strength, including grip power (Dynamometer®, TTM, Japan, for patient 1; Grip Strength Dynamometer®, Takei, Japan, for patients 2–5) and pinch power (PinchTrack™, Jtech, Japan), was assessed every 2 weeks. The Barthel index and gross motor function measure manual (GMFM) were assessed every 6 months from the second year (Hosoda and Yanagisawa 2000; Kondo and Fukuda 2000). Occlusal force in the right and left first molar was measured using the Occlusal Force Meter GM10® (Nagano Keiki, Japan) every 6 months. In this test, which was repeated three times, patients were asked to bite on a block as hard as possible. All patients rested for more than 2 h before each muscle strength test. Normal values for grip power

Table 1 Baseline patient characteristics and conditions

Patient no.	1	2	3	4	5
Sex	Male	Male	Female	Female	Female
Age at inclusion (years)	66	55	44	38	32
Age at onset (years)	35	35	25	8	7
Observation period (weeks)	104	104	104	104	104
Symptom at onset (weakness)	Lower extremities	Lower extremities	Lower extremities	Neck	Lower extremities
Ventilator since (age in years)	58	49	36	32	21
Duration of ventilator use (years)	8	7	8	6	11
Wheelchair-bound	Complete	Complete	Complete	Complete	Partial
Ventilator use (h/day)	24	10 (at night)	24	22	10 (at night)
Tracheotomy (age in years)	None	48	36	None	None
Wheelchair since (age in years)	51	48	36	36	29
Genotype	c.1585–1586TC > GT(p.S529V) homozygote	c.546 G > T(p.T182T) homozygote	c.307 T > C(p.C103R)/ c.546 G > A(p.T182T)	c.1309 C > T(p.R437C)/ c. 1857 C > G(p.S619R)	c.546 G > T(p.T182T)/ c.1798 C > T(p.R600C)
Enzyme activity[a]	1.2 (M)	0.6 (M)	1.88 (M)	0.46 (F)	3.8 (M)
Complications	Diabetes mellitus	Atrial fibrillation	Interstitial pneumonia pneumothorax	Pneumothorax subcutaneous/ mediastinal emphysema	—
Pathology	Myopathic changes	Myopathic changes	Myopathic changes	Myopathic changes	Myopathic changes
AcP- and PAS-positive vacuoles	Few	Scattered	Scattered	Stained for acid phosphatase	Many

[a] *(M)* Muscle (nmols 4MU/mg/h) (14.6±4.4), *(F)* fibroblast (mmol/pg protein) (161±32.4)

and occlusal force were provided by the manufacturer, and three healthy volunteers were tested as controls for pinch power [see Table in Electronic Supplementary Material (ESM)]. Blood cell counts and blood chemistry tests were conducted regularly. We interviewed patients and their families about activities of daily living (ADL). IgG antibodies to rhGAA were measured regularly by enzyme-linked immunosorbent assay (ELISA) (Kishnani et al. 2006).

Annual changes in quantitative parameters (pulmonary function tests, grip power, pinch power, and occlusal force) were calculated for the first and second years by subtracting old data from new data. Changes were analyzed with the Mann-Whitney *U* test. Statistical analyses were performed with SPSS for Macintosh (version 18, SPSS, Chicago, IL).

Results

Case presentation

Patient 1 suffered from limb muscle atrophy at age 35. He could not climb stairs and visited us at age 44. Muscle biopsy and acid maltase activity revealed Pompe disease. He lost ambulation at age 51. He experienced dyspnea, and %VC was 22.4 at age 58. Nocturnal NIV was initiated; he required continuous NIV from age 63 and was able to remove the NIV mask for <1 min before ERT. ERT was initiated at age 66. After 6 months of ERT, the patient was able to stop NIV for 9 min, allowing for a much easier transfer of the patient from car to wheelchair by the caregiver. This also provided the caregiver more than 5 min for shaving and/or cleaning the patient's face, compared to the 1-min limit before ERT.

Patient 2 had difficulty climbing stairs from age 36. He experienced dyspnea in the supine position at age 47 and visited a physician due to morning headache and severe dyspnea. He presented with pneumonia and CO_2 narcosis; nocturnal oxygen therapy was initiated after recovery. A muscle biopsy led to the diagnosis of Pompe disease. The patient lost ambulation during hospitalization. He visited us at age 50 and nocturnal NIV was initiated. The patient had difficulty lying down in the supine position without NIV before ERT. After ERT was initiated at age 55, he was able to lie down for 10 min at 24 weeks of ERT and for 60 min at 48 weeks without respiratory support. He was also less fatigued in the afternoons and able to drive alone for 2 h after 40 weeks.

Patient 3 noticed gait disturbance at age 22, visited a neurologist at age 26, and was diagnosed with limb-girdle

muscular dystrophy. At age 36, she complained of morning headache and drowsiness; she was intubated and tracheostomy was performed due to CO_2 narcosis and pneumonia. The patient lost ambulation during hospitalization and had recurrent pneumothorax and pneumonia. She visited us at age 39 and was diagnosed with Pompe disease by muscle biopsy and GAA activity. Recurrent pneumonia due to *Pseudomonas aeruginosa* required hospitalization with intravenous antibiotics once every 2 months before ERT. After ERT was initiated at age 44, she developed a mild fever of <38°C twice at 12 and 36 weeks after ERT, and recovered without antibiotics. She was able to open a plastic bottle unaided after 24 weeks of treatment, a task that could not be completed for 8 years prior to treatment. She was able to easily move from bed to wheelchair after 44 weeks. She also noticed less fatigue during meals, was able to pull up both legs unaided after 2 years of ERT, and could put on socks while sitting in the wheelchair.

Patient 4 had proximal weakness at age 15. She was referred to a neurologist and found to have high creatine kinase levels (1,256 U/L) and mild respiratory dysfunction (%VC: 77) at age 21. She was diagnosed with late-onset Pompe disease by muscle biopsy and fibroblast acid maltase activity. At age 32, she experienced dyspnea and initiated NIV during the night. At age 35, her %VC decreased to 18.9 and she required NIV all day. She began to use a wheelchair due to exertional dyspnea. At age 36, she presented with a right-sided pneumothorax, and %VC decreased to 15.8. She was able to turn off NIV only for 5 min to take a bath and could not comb her hair by herself before ERT. At 24 weeks after ERT initiation, pinch power increased from 48.4 N to 55.2 N, and she was able to stand with less effort. At 64 weeks of treatment, she was able to switch off NIV for 15 min while taking a bath and combing her hair. However, she experienced severe dyspnea and recurrent pneumothorax after 64 weeks of ERT and became fully dependent on NIV thereafter. She developed pneumothorax and emphysema at 80 weeks of ERT again and was completely bedridden and required cuirass ventilation in addition to NIV. She was also treated with parenteral hyperalimentation, including standard calorie and protein, for approximately 1 month due to inability to eat caused by dyspnea. After recovery from severe emphysema, she remained bedridden and consequently lost ambulation. Occlusal force was also lower after parenteral hyperalimentation.

Patient 5 could not stand without hand support and visited a pediatrician at age 13 and visited us and muscle biopsy and acid maltase activity. She initiated NIV at age 21 and required a wheelchair at age 29. After ERT was initiated at age 31, she found it easier to expectorate sputum through coughing than before ERT and could move her hip from floor to chair unaided after 44 weeks, which had been impossible for several years. She also noticed alleviation of lumbago, and after three doses of ERT, she was able to discontinue non-steroidal anti-inflammatory drugs (NSAIDS) used for back pain. The patient suffered from emaciation before ERT and was advised that this could not be resolved, but she gained 3 kg of body weight after ERT. At present, she can drive 2.5 h to go to the hospital every 2 weeks, which was impossible before ERT due to fatigue and back pain.

ERT-induced changes

Table 2 lists the results of clinical and laboratory tests before and after ERT. The mean duration of follow-up was 104 weeks. Grip power (Fig. 1a) and pinch power (Fig. 1b) showed gradual improvement in all patients. In patient 4, both grip and pinch powers continued to improve until 60 weeks after ERT initiation, but deteriorated thereafter. Occlusal force improved markedly in patients 1 and 3 (Fig. 1c), but deteriorated in patient 4. No changes in MMT were noted in any of the patients. GMFM improved slightly in patients with a score of >25, while it remained unchanged in those with a score of <5. After initiation of ERT, all patients, except patient 4 who had severe emphysema and pneumothorax, showed improvement in %VC (Fig. 2a), PEF (Fig. 2b), PCF (Fig. 2c), %FVC (Fig. 2d), and/or FEV1.0 (Fig.2e).

Creatine kinase (CK) levels decreased during treatment in patients 2, 4, and 5, and particularly in patient 4 (Table 2). CK levels were normal in patients 1 and 3 at the commencement of treatment and did not show marked changes during and after treatment. Body weight [44.4 (17.0) to 43.6 (16.1) kg, $p=0.93$)] and lean body mass [25.8 (7.9) to 25.8 (10.2) kg, $p=0.99$] did not change.

Changes in the first year were greater than in the second year (Table 3). Most data were not available for patient 4 at the first year evaluation because bed rest was required for pneumothorax therapy. Changes in %VC, %FVC, PEF, PCF, pinch power, and occlusal force were greater in the first year than in the second year ($p<0.05$). While %VC, % FVC, PEF, PCF, pinch power, and occlusal force significantly changed in the first year after ERT, changes in these parameters were not significant in the second year.

IgG antibody against Myozyme® was measured in patients 1, 3, 4, and 5 (see figure in ESM). All patients were IgG antibody positive at around weeks 12 to 16, but patients 4 and 5 became negative thereafter. Furthermore, IgG antibody titers increased to a peak level in patient 3, and increased in patient 1 to 25,600. The antibody titer of patient 2, measured once at 108 weeks after ERT, was negative. Only patient 3 developed a skin rash immediately after Myozyme® infusion at 12 weeks, but the rash disappeared completely after treatment with an antihistamine. Other patients did not experience any infusion-related reactions.

Table 2 Results of clinical and laboratory tests before and after ERT

		Patient 1			Patient 2			Patient 3			Patient 4			Patient 5		
		Pre	1 year	2 year	Pre	1 year	2 year	Pre	1 year	2 year	Pre	1 year	2 year	Pre	1 year	2 year
MMT	Neck flexion	1	1	1	2	2	2	2	2	2	2	2	2	2	2	2
	Shoulder flexion	1	1	1	2	2	2	2	2	2	2	2	2	2	2	2
	Shoulder abduction	1	1	1	2	2	2	2	2	2	2	2	2	2	2	2
	Elbow flexion	1	1	1	3	3	4	3	3	3	4	4	4	3	4	4
	Elbow extension	1	1	1	4	4	4	4	4	4	4	4	4	3	3	3
	Wrist flexion	4	4	4	5	5	5	5	5	5	4	4	4	5	5	5
	Hip flexion	1	1	1	2	2	2	2	2	2	2	2	2	2	2	2
	Knee flexion	1	1	1	2	2	2	2	2	2	3	3	3	2	2	2
	Knee extension	1	1	1	2	2	2	2	2	2	3	3	3	2	2	2
	Ankle flexion	1	1	1	5	5	5	2	2	2	4	4	4	5	5	5
Body weight (kg)		44	43	43	73.0	70	69	42	40	42	33	31	31	30	31	33
Lean body mass (kg)		23.9	22.6	22.6	39.8	39.8	39.8	23.0	24.4	24.4	21.1	NT	19.9	21.4	22.2	22.2
Pulmonary function	%VC	4.9	10.7	9.6	45.6	62.0	67.2	12.1	15.4	17.3	17.6	NT	9.2	13.1	19.5	21.4
	%FVC	0.0	26.8	7.7	46.3	51.2	66.1	9.3	12.5	16.1	14.2	NT	7.0	10.3	17.7	20.4
	FEV1.0	0.00	0.62	0.21	1.52	1.78	1.99	0.24	0.49	0.41	0.32	NT	0.14	0.29	0.50	0.55
	PEF (L/s)	0.38	0.93	0.50	3.72	6.40	5.49	0.46	0.63	0.70	0.58	NT	0.25	1.24	1.63	1.70
	PCF (L/s)	0.34	0.74	0.69	4.87	7.26	7.16	0.60	0.82	0.85	1.52	NT	0.86	1.19	1.96	2.17
Grip power (kg)		3.4	4.1	4.4	39.6	42.7	44.1	14.2	17.4	16.5	17.0	18.0	17.7	17.5	23.9	25.0
Pinch power (N)		14.7	21.1	15.5	81.9	96.1	98.8	23.6	42.4	42.5	48.3	56.3	53.0	44.3	48.5	47.3
Occlusal force (kgf)		6.4	15	15.9	NT	50.0	55.2	24.1	42.8	46.3	16.4	NT	8.4	NT	65.8	64.0
GMFM		NT	3	3	NT	25	31	NT	5	5	NT	56	59	NT	32	35
CK (IU/l)		47	36	50	238.0	132	10	166	132	100	621	NT	154	241	161	166
Barthel index		20	20	20	75.0	75	75	55	55	55	80	80	70	80	80	80

%VC Percent vital capacity, *%FVC* percent force vital capacity, *FEV1.0* forced expiratory volume in the first second, *PEF* peak expiratory flow, *PCF* peak cough flow, *GMFM* gross motor function measure, *CK* creatine kinase, *NT* not tested

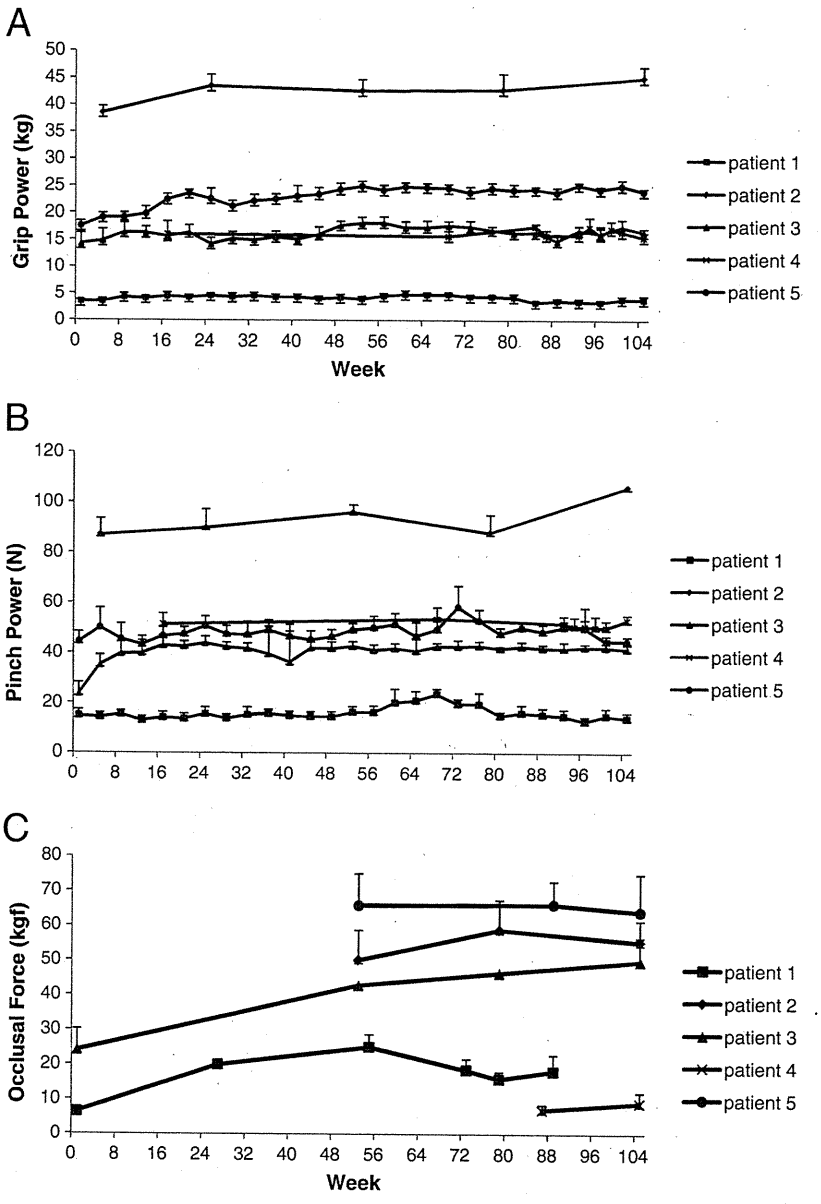

Fig. 1 Effects of ERT on grip power (**a**), pinch power (**b**), and occlusal force (**c**). Each data point represents the average of three bilateral measurements. ERT improved all of these parameters in four of five patients (with the exception of patient 4). Data are presented as mean ± SEM

Discussion

ERT is often difficult to initiate in the early stages of subclinical GSDII or in early-stage GSDII because the disease is difficult to diagnose due to heterogeneity in clinical presentation and overlapping symptoms with other neuromuscular diseases. Accordingly, it is important to gain an understanding of ERT efficacy in patients with advanced GSDII. Our study demonstrated that ERT is effective for 2 years without severe complications in adult patients who have advanced GSDII and are dependent on ventilator and wheelchair support. During the 2 years of ERT, all patients showed some improvements in muscle and pulmonary function and ADL.

All parameters improved during the first year of treatment. While the results of various tests in the second year were lower than those recorded at the end of the first year, they were still better than before ERT initiation. Although the rate of improvement differed widely among patients, our results indicate that ERT is more effective in the first year and it maintains its efficacy for 2 years. At present, there is no explanation for the better outcome in the first year compared to the second year. Taking into consideration the muscle pathology associated with GSDII, intracellular accumulation of large amounts of glycogen may cause displacement, replacement, or compression of normal cellular organelles. Thus, ERT may normalize cell function by reducing such accumulation in surviving